

Deformation Analysis and Fixture Design of Thin-walled Cylinder in Drilling Process Based on TRIZ Theory

Fulin WANG^{1*}, Bo SHENG², Yongwen WU¹, Jiawang LI¹, Zhou XU², Zhaoxia ZHU²

1. College of Mechanical and Vehicle Engineering, Hunan University, Changsha, Hunan;
2. AECC South Industry Limited company, Zhuzhou, Hunan

***Corresponding Author:** Fulin WANG, College of Mechanical and Vehicle Engineering, Hunan University, Changsha, China; wangfulin_01@163.com

Abstract:

Thin-walled cylindrical workpiece is easy to deform during machining and clamping processes due to the insufficient rigidity. Moreover, it's also difficult to ensure the perpendicularity of flange holes during drilling process. In this paper, the element birth and death technique is used to obtain the axial deformation of the hole through finite element simulation. The measured value of the perpendicularity of the hole was compared with the simulated value to verify then the rationality of the simulation model. To reduce the perpendicularity error of the hole in the drilling process, the theory of inventive principle solution (TRIZ) was used to analyze the drilling process of thin-walled cylinder, and the corresponding fixture was developed to adjust the supporting surface height adaptively. Three different fixture supporting layout schemes were used for numerical simulation of drilling process, and the maximum, average and standard deviation of the axial deformation of the flange holes and their maximum hole perpendicularity errors were comparatively analyzed, and the optimal arrangement was optimized. The results show that the proposed deformation control strategy can effectively improve the drilling deformation of thin-walled cylindrical workpiece, thereby significantly improving the machining quality of the parts.

Keywords: Thin-walled cylindrical parts; Fixture; Deformation analysis; Drilling; TRIZ theory

1 Introduction

The thin-walled cylindrical parts made by high-temperature alloy have been widely used in the aerospace due to their compact structure, high specific strength and high temperature resistance. However, the thin-walled cylindrical parts have weak rigidity and poor processing characteristics, which make them easily deformed during the manufacturing process, and it is difficult to guarantee the machining accuracy. Therefore, it is of great significance to analyze and control the deformation of this typical kind of parts during machining. Some methods are commonly used to control deformation of parts, such as improving the structural machinability of the workblank, improving the fixture scheme, revising the tool path, and optimizing the process parameters, etc [1-8]. Among them, with properly positioning, clamping and supporting of the parts, the deformation can be effectively reduced, and the processing quality of the parts can be improved.

So far, many experts and scholars have carried out comprehensive study on the deformation control and the drilling quality of thin-walled parts, and also have achieved

some research results. Wang et al. [9] established a finite element optimization model for the milling of thin-walled arc-shaped parts. With optimizing the clamping position, the elastic deformation in machining of the part was reduced. The influence of three factors such as clamping position, clamping order and loading method on the deformation of frame-type thin-walled parts in the clamping process was simulated by Dong et al. [10], and the optimal clamping scheme was selected. Qin et al. [11] analyzed the clamping deformation generated by different clamping order and position of location, optimized the clamping scheme based on the neural network and genetic algorithm, which effectively reduced the deformation of thin-walled parts. Necmettin [12] developed an improved genetic algorithm to optimize the layout of fixtures, the result showed that the deformation of part and the computational cost were obviously cut down. Selvakumar et al. [13] proposed an experimental design algorithm based on an artificial neural network to acquire the optimal fixture layout, and the maximum elastic deformation of designed part caused by the clamping force and cutting force was reduced. Croppi

et al.^[14] proposed a fixture optimization method for drilling thin-walled parts. Based on the workpiece geometry and tool path, the optimal fixture design is obtained through the combination of finite element model, geometric error model and chatter model.

It is difficult to ensure the machining accuracy by the general drilling and clamping method for thin-walled cylindrical parts. The trial and error method is generally used in fixture design, which is inefficient and ineffective. At present, the theory of inventive problem-solving (TRIZ) has been introduced into the field of fixture design by researchers. Ren et al.^[15] proposed the innovative design of reconfigurable fixture based on TRIZ conflict resolution principle. Huang et al.^[16] combined axiomatic design (AD) theory with inventive problem solving (TRIZ) theory, and proposed an axiomatic design method of machining fixture scheme integrating TRIZ. The design of adaptive support fixture for thin-walled cylinder parts based on TRIZ theory in drilling process can improve the efficiency of fixture design process and enhance the scientificity of design process.

In this paper, finite element simulation analysis was performed on drilling of the flange of thin-walled cylindrical part. An adaptive fixture is developed based on TRIZ theory, which can enhance the stiffness of the parts, and thus significantly reduce the hole perpendicularity error caused by drilling deformation.

2 Drilling deformation analysis

The structure of a thin-walled cylindrical part is shown in Fig. 1. The material of part is a nickel-base superalloy and the cylinder diameter is 384 mm. The upper flange has a width of 18 mm and a thickness of 3.5 mm. The flange has a circumferential hole system with 46 small holes and four grooves. The diameter of these holes is 5 mm and the distance between the hole centers and the outside of the cylinder wall is 13 mm. The perpendicularity errors of these flange holes based on the bottom end surface of the cylindrical part are $\Phi 0.035$ mm. However, the perpendicularity of holes is out of tolerance after processing.

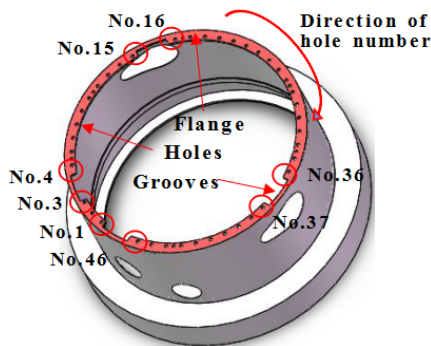


Fig. 1 The structure of a thin-walled cylindrical part

The ratio of diameter to thickness of the flange is up to 110, which is a typical weak stiffness structure. The grooves divide the flange into four independent plates with different sizes, so that the flange is easily deformed when subjected

to an axial force, which further reduces the rigidity of the flange. Therefore, there is a strong correlation between the poor hole perpendicularity on the flange and processing deformation of the flange.

2.1 Finite element analysis of drilling deformation

The drilling process of thin-walled cylindrical part is simulated by ABAQUS software. The axial force and the torque are applied to 46 holes on the flange in turn. In order to simulate the actual processing condition, each force is exerted on different analysis step, and the element birth and death technique is used to remove the material in holes with the axial force adding gradually. According to the material parameters of the parts and processing parameters, it can be deduced that the drilling axial force is 152 N, and the drilling torque is 1 N·m with the formula for drilling theory^[17].

Fig. 2 shows the deformation cloud image of the part during drilling the first hole. It is seen that the cylinder wall is circumferential closed structure, and the deformation of the cylinder produced by the drilling wall is much smaller than the deformation of the flange. The maximum deformation occurred near the edge of the first hole with the value of 0.61 mm. Since the drilling force acts perpendicularly on the flange end surface, the axial deformation of the flange is much larger than the tangential deformation and radial deformation. The axial deformation at the center of each small hole is shown in Fig. 3. It is seen that the deformation of these holes (Hole No.1, No.3, No.4, No.15, No.16, No.36, No.37, and No.46) at the edge of the groove shows a local peak because the groove makes the rigidity at these small holes worse.

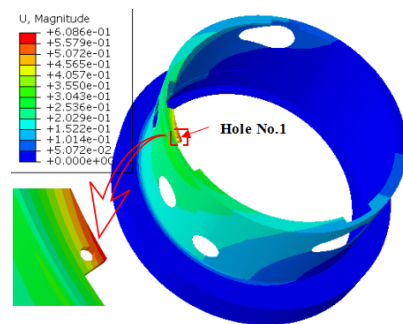


Fig. 2 The deformation during drilling the first hole

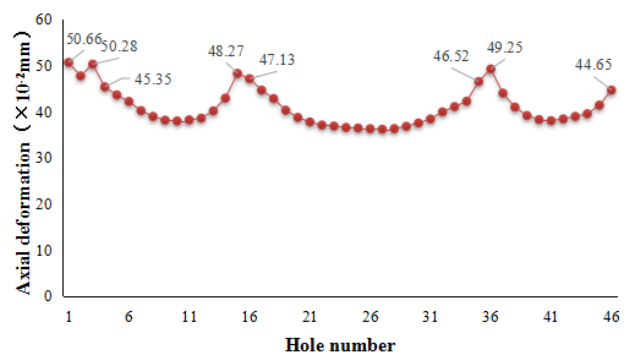


Fig. 3 The axial deformation at the center of each hole

2.2 Simplified calculation of hole perpendicularity error

Since the deformation of the cylinder wall is relatively small, the side of the flange near the cylinder wall is approximately considered as a fixed constraint. Under the action of the drilling force, the flange is bent and deformed.

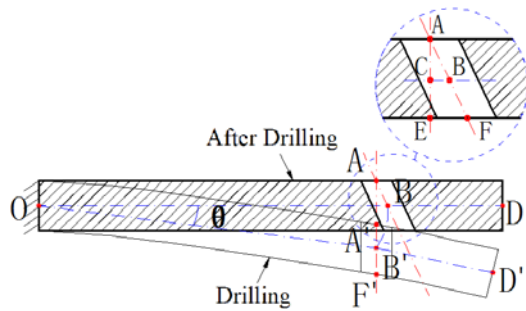


Fig. 4 The schematic diagram of drilling deformation of the flange

The drilling axial force initially acts at point A, and during the drilling process, the tool is regarded as a rigid body. Therefore, the drilling action point is always on the same vertical line. After drilling, the point A', B', F', and D' will return to the point A, B, F, and D, respectively. A'F' and AF are the centerline of the hole during drilling and after drilling. OD' and OD are the centerline of the thickness of the flange section during drilling and after drilling. The point B' is the intersection of A'F' and OD', and point B is the intersection of AF and OD. The point E is the intersection of the vertical line through the point A after drilling and the bottom edge of the flange section. The point C is the intersection of AE and OD.

As the elastic deformation disappears, the central axis of the hole is inclined. As a result that the center layer is not stretched or compressed after drilling, the lengths of the line OB and the line OB' are equal. In the case of small deformation, the line OB' can be approximated as a straight line. According to their geometric relations, the lengths of line CB and line EF can be expressed as:

$$l_{CB} = l(\sec \theta - 1) \quad (1)$$

$$l_{EF} = 2l_{CB} \quad (2)$$

Where l is the horizontal distance of the line OA, which is the radial distance between hole center and cylinder wall; θ is the angle between the line OB and OB'. Then

$$\theta = \arctan(h/l) \quad (3)$$

Where h is the vertical distance between point B and B', which can be regarded as the axial deformation of flange at holes.

The simplified calculation formula for the perpendicularity error of hole caused by the elastic deformation of flange is as follows:

$$t = 2l_{EF} = 4l(\sec \theta - 1) \quad (4)$$

2.3 Comparison of the perpendicularity errors

In the corresponding analysis step of the finite element

simulation model, the axial deformation at the center of the hole is obtained. The perpendicularity error of each small hole can be obtained by equations (3) and (4). Due to the large deformation of the eight small holes at the edge of the groove, the perpendicularity errors of these special small holes are selected for analysis. The measured value of the perpendicularity error is obtained under the Coordinates Measuring Machine (CMM), and the comparison between measured and simulated values is shown in Fig. 5. The simulated value ranges from 0.031 mm to 0.039 mm, and the measured value varies from 0.037 mm to 0.047 mm. The relative error is between 9.3% and 18.2%, and the average relative error is 14.0%. Compared with the vertical error simulation value and measured value of each hole, the simulation value is less than the measured value. In the actual drilling process, the verticality of the hole is affected by machine vibration, drilling heat and other factors. In the drilling simulation, these factors are simplified, and the influence of the main factors of drilling force and torque is only considered, so there was a certain error between the simulation value and the measured value.

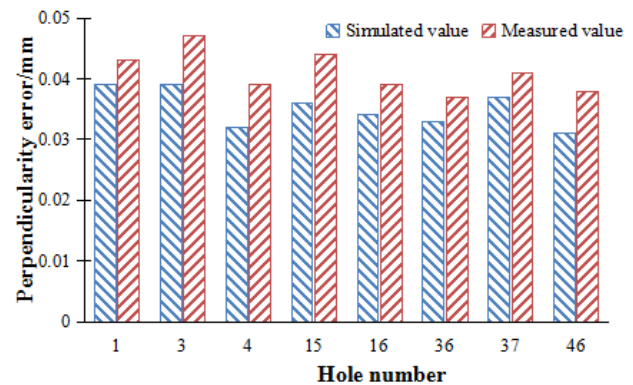


Fig. 5 The comparison of the perpendicularity errors

3 Design of fixture scheme based on TRIZ theory

Since the thin-walled cylindrical workpiece is easy to deform during the drilling process, a special fixture is necessary to reduce deformation.. TRIZ is a theory for product innovation design, which systematically put forward solutions to problems in design and effectively solve various conflicts in product design.

3.1 Analysis of deformation based on TRIZ theory

The case shell needs to be clamped in the drilling process. Since the casing is a weak rigid part, too large clamping force will lead to deformation of the workpiece, on the other hand, too small clamping will lead to vibration of the workpiece. Therefore, in order to ensure the position of the cylinder end flange in the drilling process, it is necessary to provide appropriate clamping force. Improving clamping force requires changing fixture structure, which will increase system complexity. The contradictory parameters and the original understanding of the invention can be obtained by TRIZ analysis, as shown in Table 1.

Table 1 Contradiction matrix

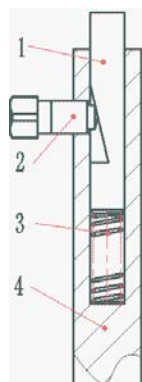
Improved parameters	Deterioration parameters	the principle of invention
Clamping force (10 Force)	Complexity of clamping system (36 Complexity of system)	Principle 10 : Prior action; Principle 18 : mechanical vibration; Principle 26 : replication; Principle 35 : Changes in physical or chemical parameters

As shown in Table 1, Principle 10 refers to pre-action and auxiliary supports can be designed to provide pre-support for thin-walled cylinder parts to improve the stiffness of the workpiece. Principle 18 refers to mechanical vibration. According to this principle, a spring shock absorber is designed to reduce vibration during drilling process. Principle 26 refers to duplication. Replaceable fixture parts are used in the design of the drilling fixture, and the cost is reduced by copying and replacing the fixture parts that are easy to wear. Principle 35 refers to the change of physical or chemical parameters, namely the redesign of the original structure, which is not applicable to the solution of this problem and can be ignored.

3.2 Fixture design based on TRIZ

According to the above solutions, To reduce the verticality error of the small holes in the flanges of thin-walled cylinder parts, an adaptive support fixture scheme was proposed. The structure of the adjustable self-adaptive support fixture is shown in Fig. 6. The fixed support rod 4 is connected to the base of the fixture and keeps relatively fixed. When the setting screw 2 is not tightened, the spring 3 is in a compression state under the action of the gravity of the workpiece and the movable support rod 1. Tighten the locking screw 2, can make the movable support rod 1 fixed.

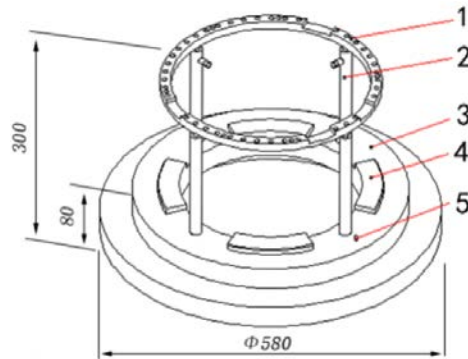
In this way, the supporting fixture and the inner surface of the workpiece are always attached to each other, so as to provide better support, increase the process stiffness of the workpiece, and reduce the axial deformation caused by drilling force in the processing process.



1. Movable support rod 2. Set screw 3. Spring 4. Fixed support rod

Fig. 6 The support rod of fixture

The overall design of the fixture is shown in Fig. 7. The assembly of the parts and fixtures is shown in Fig. 8. The support structure consists of a support ring 1 and four support bars 2. There are 46 avoidance holes and four avoidance grooves on the support ring. The fixture is located inside the thin-walled cylinder.



1. Support ring 2. Support rod 3. Pedestal 4. Limit pin

Fig.7 The fixture structure

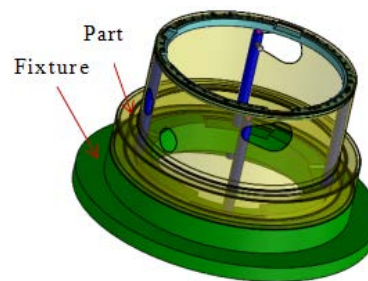


Fig. 8. The 3D assembly model of part and fixture

3.3 Numerical analysis of drilling deformation

To reduce the perpendicularity error, the axial deformation of flange must be controlled. In order to meet the requirements of processing accuracy and simplify the operation, the bottom surface of the flange needs to be tightly supported by an adaptive support fixture. When the fixture is vacant, the simplified force model is shown in Fig. 6, and the distributed force q is generated by the gravity F_1 of the support ring itself. The support ring gravity F_1 and the spring force F_3 reach a force balance. The equation is shown as follows:

$$F_1 - 4F_3 = 0 \tag{5}$$

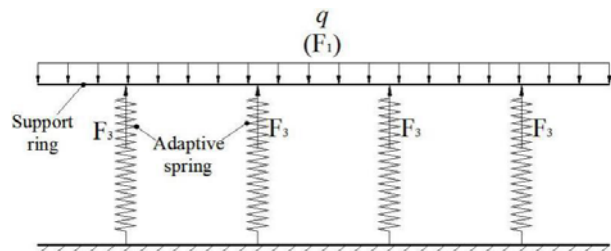


Fig. 6 Simplified force model when the fixture is vacant

When not processed, the simplified force model of the fixture is shown in Fig. 7. The distributed force q is generated by the gravity F_1 of the support ring itself and the force F_2 transmitted from the casing gravity G to the support ring. F_1 , F_2 and the spring force F_3 reach a force balance. The equation is shown in Equation 6.

$$F_1 + F_2 - 4F_3 = 0 \quad (6)$$

where, $F_2 \leq G$.

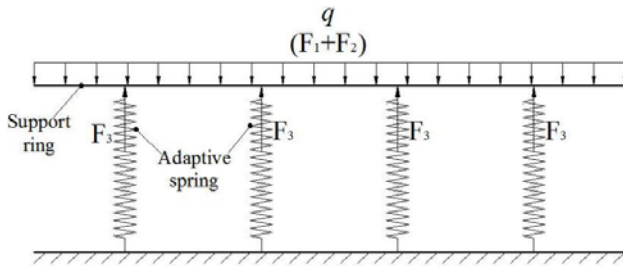


Fig. 7 Simplified force model of when not processed

According to Hook's law:

$$F_3 = k\Delta x \quad (7)$$

where, k is the spring stiffness and Δx is the deformation of the spring.

The change range of the spring deformation Δx is:

$$\frac{F_1}{4k} \leq \Delta x \leq \frac{F_1 + F_2}{4k} \quad (8)$$

when $F_2 = G$, there is

$$(\Delta x)_{\max} = \frac{F_1 + G}{4k} \quad (9)$$

At this time, the spring force is just balanced with the weight of the support ring and the weight of the casing, which is ideal.

The maximum working stroke h of the designed spring:

$$(h)_{\max} = \frac{G}{4k} \quad (10)$$

In this paper, the gravity of the casing is about $G = 108N$, so the maximum working stroke of the spring and its stiffness need to meet:

$$(h)_{\max} = \frac{27}{k} \quad (11)$$

4 Optimization of support layout

The position distribution of four support rods in the fixture affects the overall deformation of part. According to the idea of the uniform distribution of the support structure and the targeted support at the weak rigidity, three schemes are proposed for the position distribution of the support rods (as shown in Fig. 11). In Scheme 1, four support rods are respectively placed under the Hole No.7, No.19, No.32, and No.44, with a distribution angle of 90° between them. In Scheme 2, four support rods are respectively placed under the Hole No.2, No.14, No.25, and No.37, with a distribution angle of 90° between them. In Scheme 3, four support rods are distributed on the weak rigid position of the thin-walled cylindrical part to achieve targeted support, which are respectively placed under the Hole No.4, No.16, No.36, and No.46.

The designed support rod has good rigidity and the deformation of the support ring and its contact area is negligible, so full restraint can be exerted to these areas. The upper surface of the support ring and the lower surface of the flange of the part are set with the contact pair, and the magnitude of load and the method of application are consistent with those of the finite element model in the case of no fixture.

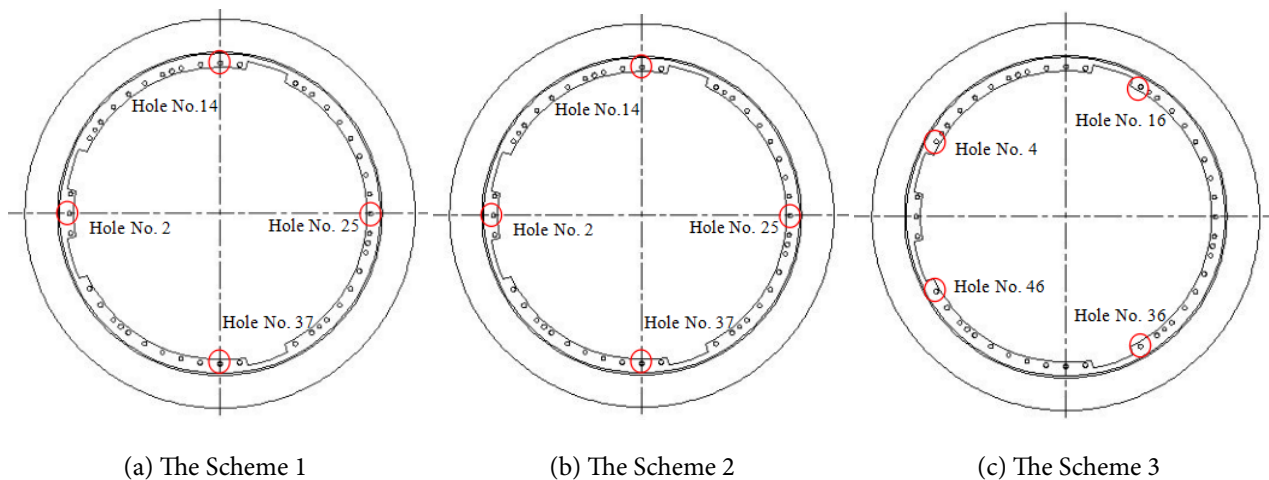


Fig. 11 The position distribution scheme of support rods

4.1 Comparative analysis of drilling deformation in different scheme

Fig. 12 show deformation distribution contours when the Hole No.1 on the flange is drilled in three

fixture supporting layout schemes. Compared with the deformation in the case of no fixture in Fig. 2, the maximum deformation was not observed near the Hole No.1 but recorded on the support ring. Due to the

different layout of the support rods, the position where the maximum deformation occurs in each scheme will be shifted to different degrees. Comparing Fig. 2 and Fig. 12,

the three fixture support schemes can reduce the maximum deformation of the part from 0.61 mm to 0.1 mm, 0.03 mm and 0.04 mm respectively when drilling the Hole No.1.

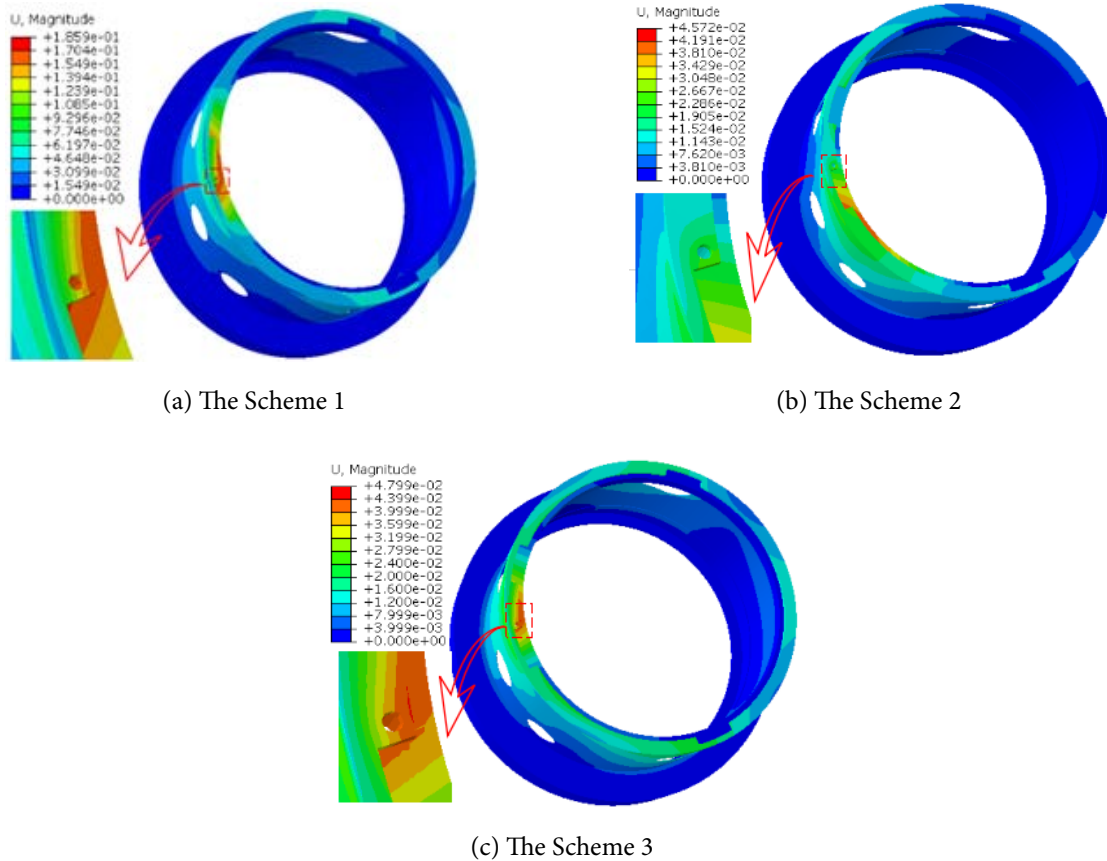


Fig. 12 The deformation distribution contours when drilling the Hole No.1 in three fixture supporting layout schemes

Fig. 13 shows the axial deformation at the center of each small hole in three fixture supporting layout schemes. It can be seen that in these schemes, the axial deformation at the center of the hole shows a wave-like undulation respectively. The main reason is that the smallest deformation of the part occurs near the support rod during drilling process, and the deformation of the part gradually increases as the drilling position deviates from the support rod.

hole center in each scheme. It can be seen that the mean value of axial deformation is 0.41 mm without fixture. The mean value of axial deformation in Scheme 1 and Scheme 2 is almost equal, decreasing to about 0.06 mm. However, the standard deviation of the axial deformation in the Scheme 2 is 1.4% smaller than in the Scheme 1, and its deformation fluctuation value is also smaller. In Scheme 3, the support rods are unevenly distributed. Its maximum axial deformation, mean value and standard deviation are 45%, 33.3% and 37% larger than those of the Scheme 2, respectively.

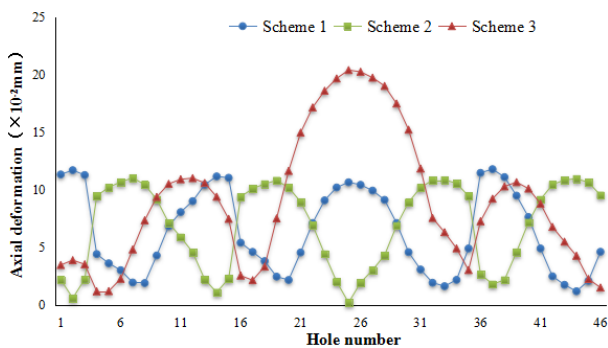


Fig. 13 The axial deformation at the center of each small hole in three fixture support schemes

Table 2 shows the comparison of axial deformation at

Table 2 The comparison of axial deformation at hole center in each scheme

	Maximum (mm)	Mean (mm)	Standard deviation
Without fixture	0.51	0.41	4.10×10^{-2}
Scheme 1	0.12	0.06	3.72×10^{-2}
Scheme 2	0.11	0.06	3.67×10^{-2}
Scheme 3	0.20	0.09	5.83×10^{-2}

4.2 Comparative analysis of the maximum perpendicularity error of holes

The maximum perpendicularity errors of the small

holes without fixture and in three fixture supporting layout schemes are calculated, as shown in Fig. 14. When there is no fixture, the perpendicularity error of Hole No.1 is the largest, which value is 3.9×10^{-2} mm. But in the other three schemes, the holes that produce the maximum perpendicularity error are Hole No.37, No.7, and No.25, respectively, and the error values are 1.5×10^{-3} mm, 1.3×10^{-3} mm, and 4.2×10^{-3} mm. Compared with the no-fixture scheme, the machining quality of the part has been improved obviously.

In Scheme 2, according to the structural characteristics of the flange surface of the part, the weak rigid position adjacent to the two grooves is taken as the starting point, and the support rods of the fixture are evenly distributed, so that the axial deformation fluctuation is small. The drilling deformation of the part is more effectively improved, and the perpendicularity error of the hole is reduced to the greatest extent. Therefore, it is determined that Scheme 2 is the optimal scheme in the proposed schemes.

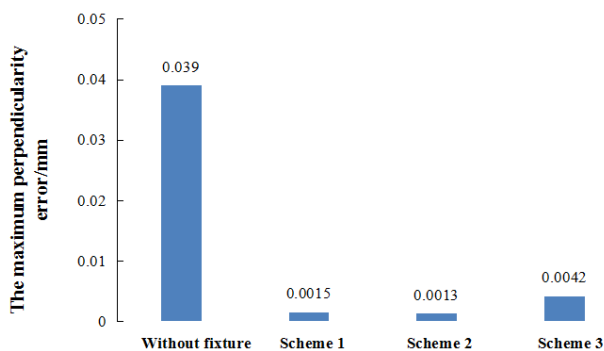


Fig. 14 The maximum perpendicularity error of holes

5 Conclusions

(1) The drilling of the flange hole of a thin-walled cylindrical part used in aerospace is analyzed by ABAQUS software. Comparing the simulated and the measured value of the perpendicularity error, the rationality of the simulation model is verified. The result shows that the drilling deformation of flange seriously affects the perpendicularity accuracy of the small hole.

(2) A drilling fixture is proposed based on TRIZ theory. The height of the supporting surface can be adjusted adaptively by the fixture. By comparing and analyzing the maximum deformation of flange in the presence or absence of fixture, it's found that the machining deformation of the thin-walled cylindrical part can enormously reduce by using the fixture, and the rationality of fixture is verified.

(3) Aiming at the position distribution of support rods in the fixture, three layout schemes are proposed and the finite element simulation is carried out. The result shows that the deformation fluctuation of scheme 2 is smallest, and the hole perpendicularity error is minimized, so that the perpendicularity accuracy of holes meets the design requirements. Therefore, the Scheme 2 is the optimal layout.

The fixture design ideas and the numerical simulation method for supporting layout optimization in this paper can provide reference for the processing deformation

control of thin-walled cylindrical parts.

References

- [1] Yin SH, Zhang Z, Hu T, et al. Experimental research on micro-drilling applying turbine-driven air spindle [J]. Journal of Hunan University: Natural Sciences 2017; 44(8): 1-7.
- [2] Zhen LY, Wang SC. Approaches to improve the press quality of thin-walled part in NC machining [J]. Acta Aeronautica ET Astronautica Sinica 2001; 05: 424-428.
- [3] Wan XJ, Hua L, Wang XF, et al. An error control approach to tool path adjustment conforming to the deformation of thin-walled part [J]. International Journal of Machine Tools and Manufacture 2011; 51(3): 221-229.
- [4] Scippa A, Grossi N, Campatelli G. FEM based Cutting Velocity Selection for Thin Walled Part Machining [J]. Procedia CIRP 2014; 14: 287-292.
- [5] Ivanov V, Mital D, Karpus V, et al. Numerical simulation of the system "fixture-workpiece" for lever machining [J]. The International Journal of Advanced Manufacturing Technology 2017; 91(1-4): 79-90.
- [6] Karuppanan B R C, Saravanan M. Optimized sequencing of CNC milling toolpath segments using metaheuristic algorithms [J]. Journal of Mechanical Science and Technology 2019; 33(2): 791-800.
- [7] Xiao GJ, Huang Y. Adaptive belt precision grinding for the weak rigidity deformation of blisk leading and trailing edge [J]. Advances in Mechanical engineering 2017; 9(10).
- [8] Emel K, Babur O. Optimization of machining parameters during micro-milling of Ti6Al4V titanium alloy and Inconel 718 materials using Taguchi method [J]. Proceedings of the Institution of Mechanical Engineers, Part B: Journal of Engineering Manufacture 2015; 231(2): 228-242.
- [9] Wang YQ, Mei ZY, Fan YQ. Finite element optimization of machining fixture layout of thin-walled arc part [J]. Chinese Journal of Mechanical Engineering 2005; 06: 214-217.
- [10] Dong HY, Ke YL. Finite element simulation for optimal clamping scheme of thin-walled part in milling process [J]. Journal of Zhejiang University (Engineering) 2004; 01: 18-22.
- [11] Qin GH, Zhao XL, Wu ZX. Optimization of multi-fixturing layout for thin-walled part based on neural network and genetic algorithm [J]. Chinese Journal of Mechanical Engineering 2015; 01: 203-212.
- [12] Kaya N. Machining fixture locating and clamping position optimization using genetic algorithms [J]. Computers in Industry 2006; 57(2): 112-120.
- [13] Selvakumar S, Arulshri K P, et al. Design and optimization of machining fixture layout using ANN and DOE [J]. The International Journal of Advanced Manufacturing Technology 2013; 65(9-12): 1573-1586.

- [14] Croppi L, Grossi N, Scippa A, et al. Fixture Optimization in Turning Thin-wall Components[J]. *Machines*, 2019, 7(4): 68.
- [15] REN G C, TIAN C, WANG C, et al. Research on innovative design of reconfigurable fixture based on TRIZ [J]. *Modular Machine Tool & Automatic Manufacturing Technique*, 2016.
- [16] HUANG B, ZHOU LS, AN LL, et al. Configuration axiomatic design method for the machining fixtures integrating TRIZ. Chinese [J]. *Journal of Scientific Instrument*, 2017, 38(4): 1031-1040.
- [17] Yang SZ, Li B, Zhou FR. *Handbook of Machining Technologist*[M]. Bei Jing: Machinery Industry Press, 2010.